Proceedings of Engineering & Technology (PET)
pp. 149-154

International Conference on Automation, Control, Engineering & Computer Science (ACECS'15)
Proceedings - Copyright IPCO-2015

ANALYSIS OF SELF-EXCITED WOUND ROTOR INDUCTION GENERATOR AT CONSTANT FREQUENCY OPERATION

Mourad SELMI and Habib REHAOULIA
selmimourad@yahoo.fr habib.rehaoulia@essstt.rnu.tn
Department of Electrical Engineering, Laboratory research SIME, ENSIT, Tunis-Tunisia

ABSTRACT—Induction machine has become very attractive for electrical power system generator in the isolated areas. Moreover, as every system, self-excited induction generator suffers from same drawbacks. The major drawbacks are the poor voltage and frequency regulations under various prime mover speeds, excitation capacitances and load impedances perturbations. In the present work, an attempt to control the frequency under various conditions of operation has been made. Therefore, by addition of an external resistance in the rotor circuit, the frequency can be maintained constant at its rated value. For a fixed load, the stator voltage remains constant over the hall range of super-synchronous if the frequency is controlled by the external rotor resistance. For various loads, the stator voltage droops when the load current increases despite the constancy of the frequency. The simulated results are compared with same experimental points. A close agreement between the experimental and calculated points proves the effectiveness of the adopted method.

Keywords— SEIG, Induction generator, frequency control

NOMENCLATURE

SEIG	Self excited induction generator
SEWRIG	Self excited wound rotor induction generator
V	Stator terminal voltage
F	Frequency
R_1	Stator resistance
R_2'	Initial rotor resistance (referred to stator)
R_{2r}'	Total rotor resistance (referred to stator)
R_f	Core loss resistance
R_L	Load resistance
X_{1s}	Stator leakage reactance
X_{2s}'	Rotor leakage reactance (referred to stator)
X_c	Excitation capacitor reactance
X_m	Magnetizing reactance
X_L	Load reactance
I_L	Load current
I_m	Magnetizing current
I'_2	Rotor current (referred to stator)
I_1	Stator current

I. Introduction

Recent studies have shown that the installed wind power generation capacity in the world has been increasing during the last few decades. Traditionally, synchronous generators are very commonly used in conventional large-scale power plants. Thanks to their relative advantageous features over the synchronous generators, induction generators are increasingly being used in generating systems based on alternative energy sources [1-2]. These features are rugged constructed, simple, robust, less expensive and require very little maintenance. Unlike synchronous machines, induction machines can be operated at variable speeds. They do not require external power supplies to produce magnetic flux for maintaining the desired voltage at the generator terminals. Hence, they are very much suitable for remote and isolated area applications [3-4].

The three-phase induction machine with a squirrel-cage rotor or a wound rotor could work as a three-phase induction generator either connected to the utility ac power distribution line or as a self-excitation power generation mode with an additional stator terminal excitation capacitor bank [5-6]. The squirrel-cage induction machine is very attractive for small and medium power generation systems because of its low cost, robustness, and high-power density. The major drawbacks in the use of self excited induction generators are the poor voltage and frequency regulations under prime mover speed and load perturbations [7-8-9]. Relatively to squirrel cage type, little research has been devoted to the wound rotor type of the induction generator [10].

In order to improve the efficiency of the presented generator, an analysis of constant frequency operation of the self excited wound rotor induction generator will be proposed. Indeed, over a wide range of super synchronous speed the control of the frequency, by additional of external resistance in the rotor circuit, under fixed or various loading impedances will be investigated. We note that the analysis behavior of this generator is based on it's per phase equivalent circuit. In order to validate the presented method, simulated results will be compared with the corresponding experimental points. The good agreement between

ISSN: 2356-5608

experimental and calculated point prove the effectiveness of the suggested control.

II. STEADY-STATE ANALYSIS OF SEIG

Often, steady state performances of SEIG are based on per phase equivalent circuit [11-12-13]. This latter is shown in fig.1. All parameters are considered constant except the magnetizing reactance and the generator slip which vary respectively according to the saturation characteristic and the prime mover speed [14-15]. Unlike most of the published works core loss resistance is not neglected thus give more accuracy to the determined performances. In the present study, nodal admittance approach is used to analyze the self excitation process of the induction generator.

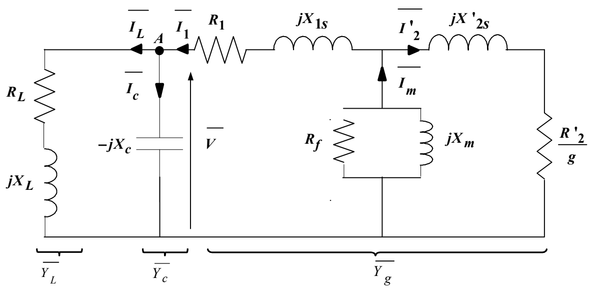

Fig1. Per phase equivalent circuit of SEIG

$\overline{Y_g}$, $\overline{Y_c}$ and $\overline{Y_L}$, can be expressed as follows:

$$
\begin{aligned}
\overline{Y_g} &= \frac{1}{R_1 + jX_{1s} + \left(\left(R_f // jX_m \right) // (jX'_{2s} + \frac{R'_2}{g}) \right)} \\
\overline{Y_c} &= \frac{1}{-jX_c} \\
\overline{Y_L} &= \frac{1}{R_L + jX_L}
\end{aligned}
\tag{1}
$$

In order to simplify the computation of the generator performances, the per phase equivalent circuit of SEIG described in fig1. Can be represented as:

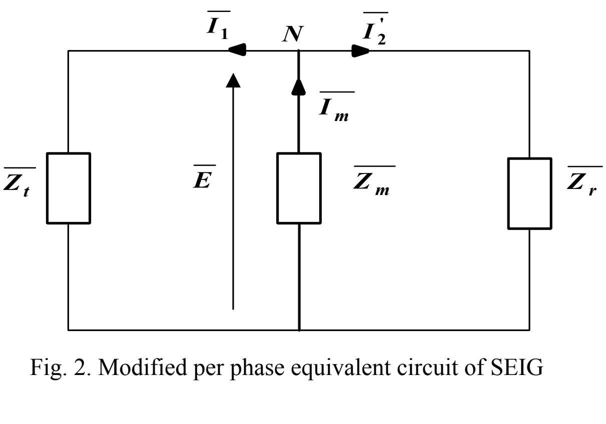

Fig. 2. Modified per phase equivalent circuit of SEIG

Where:

$$
\begin{cases}
\overline{Z_t} = ((R_L + jX_L) // \frac{1}{jC\omega}) + R_1 + jX_{1s} \\
\overline{Z_m} = R_f \; // \; jX_m \\
\overline{Z_r} = \frac{R_2^{'}}{g} + jX_{2s}^{'}
\end{cases}
\tag{2}
$$

At node "N" in fig.2 the relation between, $\overline{I_m}$, $\overline{I_1}$ and $\overline{I_2^{'}}$ can be written as:

$$
\overline{I_m} = \overline{I_1} + \overline{I_2^{'}} \tag{3}
$$

Expressions of different currents mentioned in fig. 2 are detailed in the following equations:

$$
\begin{cases}
\overline{I_m} = -\frac{\overline{E}}{\overline{Z_m}} = -\overline{E}\,\overline{Y_m} \\
\overline{Y_m} = \frac{1}{\overline{Z_m}} = \frac{1}{R_f} - \frac{j}{x_m}
\end{cases}
$$

$$
\begin{cases}
\overline{I_1} = \frac{\overline{E}}{\overline{Z_t}} = \overline{E}\,\overline{Y_t} \\
\overline{Y_t} = \frac{1}{\overline{Z_t}} = \frac{1}{((R_L + jX_L) // \frac{1}{jC\omega}) + R_1 + jX_{1s}}
\end{cases}
\tag{4}
$$

$$
\begin{cases}
\overline{I_2^{'}} = \frac{\overline{E}}{\overline{Z_r}} = \overline{E}\,\overline{Y_r} \\
\overline{Y_r} = \frac{1}{\overline{Z_r}} = \frac{1}{\frac{R_2^{'}}{g} + jX_{2s}^{'}}
\end{cases}
$$

Hence, equation (3) can be written as:

$$
\overline{E}\,(\overline{Y_t} + \overline{Y_m} + \overline{Y_r}) = 0 \tag{5}
$$

Under normal operating conditions, the stator voltage is not null. Therefore, the sum of the admittances must be equal to zero, Eq. (6).

$$
\overline{Y_t} + \overline{Y_m} + \overline{Y_r} = 0 \tag{6}
$$

$\overline{Y_t}$, $\overline{Y_m}$ and $\overline{Y_r}$ are complex values so they can be written as follows:

$$\begin{cases} \overline{Y_t} = G_t + jB_t \\ \overline{Y_m} = G_m - jB_m\,; \\ \overline{Y_r} = G_r - jB_r \end{cases} \qquad (7)$$

From equation (6) and (7) the following system can be deduced:

$$h_1(F) = G_t + G_m + G_r = 0 \qquad (8)$$

$$h_2(F, L_m) = B_t - B_m - B_r = 0 \qquad (9)$$

From equation (8), we can deduce the following expression:

$$\frac{R'_{2r}\omega}{\omega-\omega_e} = \frac{-1 \pm \sqrt{1-(2l_2\omega(G_t+G_m))^2}}{2(G_t+G_m)} \qquad (10)$$

Or, for asynchronous generator operation mode the term $\frac{R'_{2r}\omega}{\omega-\omega_e}$ is generally negative and its absolute value is much greater than the unity, consequently the solution to retain is:

$$\frac{R'_{2r}\omega}{\omega-\omega_e} = \frac{-1 - \sqrt{1-(2l_2\omega(G_t+G_m))^2}}{2(G_t+G_m)} \qquad (11)$$

Where the total resistance across the rotor winding (referred to stator) can be expressed as:

$$R'_{2r} = \left(\frac{\omega_e-\omega}{\omega}\right) . \left(\frac{1 + \sqrt{1-(2l_2\omega(G_t+G_m))^2}}{2(G_t+G_m)}\right) \qquad (12)$$

Equation (12) shows that, for a fixed load and capacitance, the total rotor resistance varied linearly in order to maintain the output frequency at a desired value.

From equation (9) we can deduce the following expression of the magnetizing inductance:

$$L_m = \frac{1 + \sqrt{1-(2l_2\omega(G_t+G_m))^2}}{B_t\omega(1+\sqrt{1-(2l_2\omega(G_t+G_m))^2}) - 2l_2\omega^2(G_t+G_m)^2} \qquad (13)$$

After L_m has been determined from equation (13), flux is calculated from the approximated polynomial of the magnetization curve. This latter is illustrated in fig3.

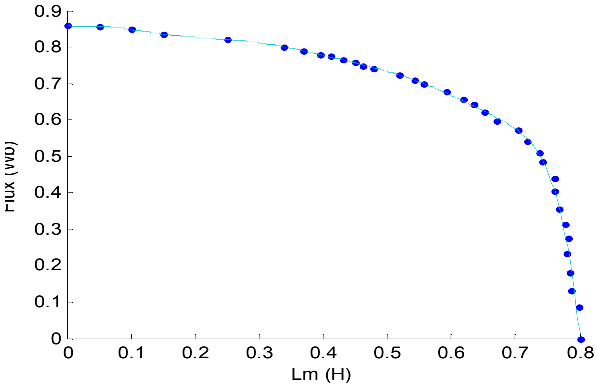

Fig. 3. Flux versus magnetizing inductance
(.experimental point, -approximated curve)

Hence, the air gap voltage can be calculated from the following expression.

$$E = \omega.Flux \qquad (14)$$

Expressions (13) and (14) implies that, for a fixed output frequency, the terminal voltages is no longer dependent of the prime mover speed and remain sensitive only to the load impedance and the excitation capacitance.

III. RESULTS AND DISCUSSIONS

In this section, the study is focused to the operation of SEWRIG at constant frequency and under various prime mover speed and load perturbations. It is assumed that in the following results, excitation capacitance is maintained constant at C=20uF. Thus, the parameters of the wound rotor induction generator used in the per phase equivalent circuit are mentioned in the following table I.

TABLE I
PARAMETER OF THE STUDIED GENERATOR

NAME	PARAMETER	VALUE
Rated power	P_N	0.8kW
Rated voltage	U_N	230/400 V
Rated current	I_N	2/3.5 A
Frequency	F	50 Hz
Pole pair number	P	2
stator resistance	R_S	8.27 Ω
Referred rotor resistance	R'r	10.45 Ω
Stator leakage reactance	X_{1S}	13.18 Ω
Referred rotor leakage reactance	X'_{2S}	13.18 Ω

A. *Constant Frequency and Fixed Load Operation*

For fixed load resistance $R_{L1} = 250\Omega$, fixed excitation capacitance and various super synchronous speeds, the variation of the stator voltage and the total rotor resistance required to maintain the frequency at its rated value are illustrated in the following figure.

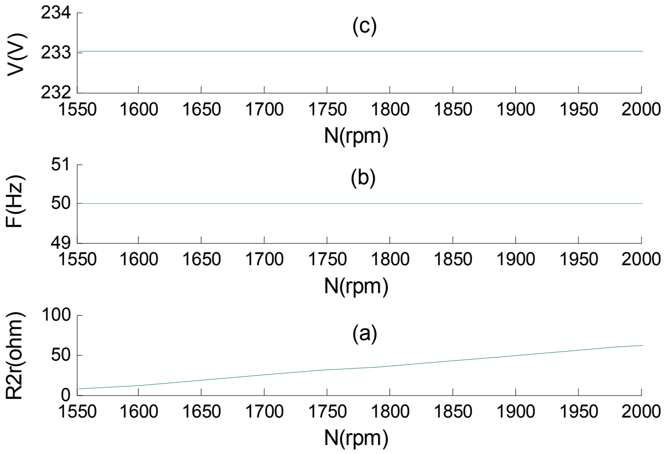

Fig.4. Variation of voltage, frequency and total rotor resistance against speed for constant frequency operation

Fig.4 (a) shows that the rotor resistance required to maintain the frequency at its rated value should be increased with the speed. While fig.(4) (b) and (c) prove the constance of the frequency and the voltage, respectively, over wide range of super-synchronous speed.

B. Constant Frequency and Two Different Loads Operation

For two resistance loads, $R_{L1} = 250\Omega$ $R_{L1} = 200\Omega$ and wide range of super-synchronous speed, evolution of the total rotor resistance, the frequency and the stator voltage against each speed have been mentioned in the following figure

.

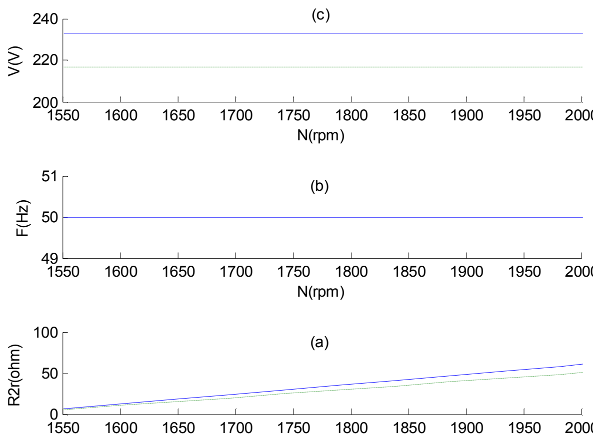

Fig. 5. Variation of voltage, frequency and total rotor resistance against speed for constant frequency operation

Fig.5.(a) shows that, for each speed, the rotor resistance required to maintain the frequency at its rated value should be decreased when the load current increase. Fig.(5) (b) prove, for each resistance load, the Constance of the frequency despite wide range of super-synchronous speed. Fig.(5) (c) shows that the stator voltage remain constant for each resistance load over the hall range of the speed. However, for RL1 the stator voltage remain constant at V1=233V. For RL2 the stator voltage reside constant at V2=218V. We note that the stator voltage drops when the load current increase.

C. Constant Frequency, fixed speed and Various Loads Operation.

The variation of the stator voltage, the frequency and the total rotor resistance against the load current are mentioned in fig. 6. Curves illustrated in fig.6 (a), show that the total rotor resistance required to maintain the frequency at its rated value decrease with the load current. Thus, fig.6 (b) proves the constancy of the frequency for the hall range of the load current and for the different considered speeds. Fig.6 (c) shows that the stator voltage drops with the load current. Indeed, the different results presented previously show that, for fixed load, the stator voltage remain independent to the prime mover speed if the frequency is kept constant by addition of external rotor resistance. Thus, when the load resistance is varied, the stator voltage drops with increasing load current. To ensure the stability of the voltage, the capacitor has to be continuously controlled.

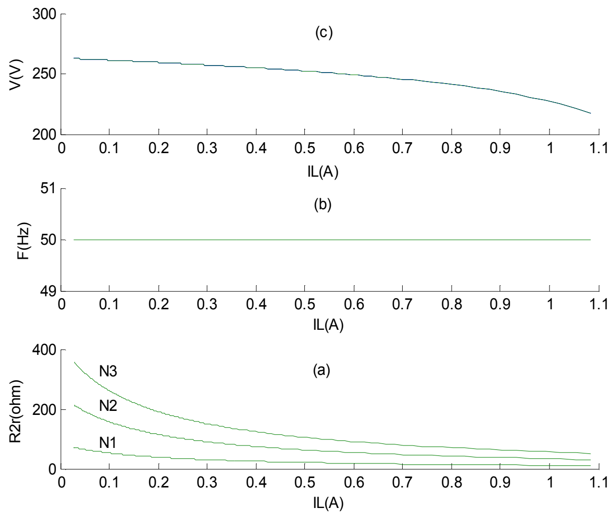

Fig. 6. Variation of voltage, frequency and total rotor resistance against load current (N_1=1600 rpm, N_1=1800 rpm et N_1=2000 rpm)

IV. Experimental Tests

In order to validate the simulated results presented above, eperimental tests have been investigated on a 0.8kW wound rotor induction generator with a fixed capacity $C = 17.5\mu F$ and fixed resistance load $R_L = 320\Omega$ available in our laboratory. The generator is coupled with a fixed load and excitation capacitance. For same prime mover speed greater than the synchronous speed, the adequate rotor resistance needed to maintain the frequency at the rated value is additionated, then the terminal voltage is measured. The different results measured are presented in fig. 7 with the corresponding simulated points.

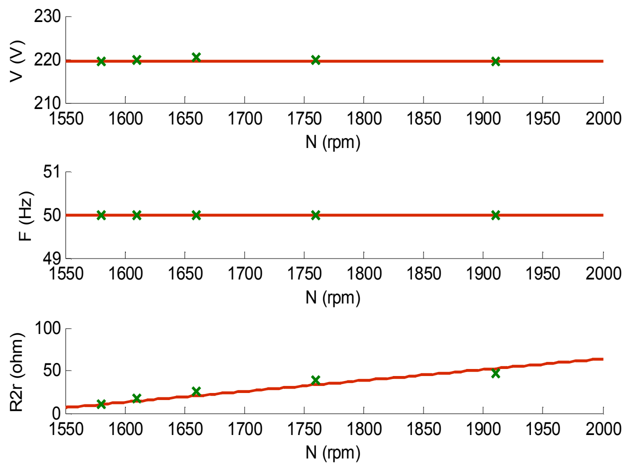

Fig. 7. Simulated results with the corresponding experimental tests for fixed load: (- simulated points, ×experimental points)

We note in the different figures illustrating the simulated and the correspondent experimental results a close agreement between the computed and experimental results which confirms the effectiveness of the adopted method.

The experimental points are determined throughout the following experimental bench, fig.8.

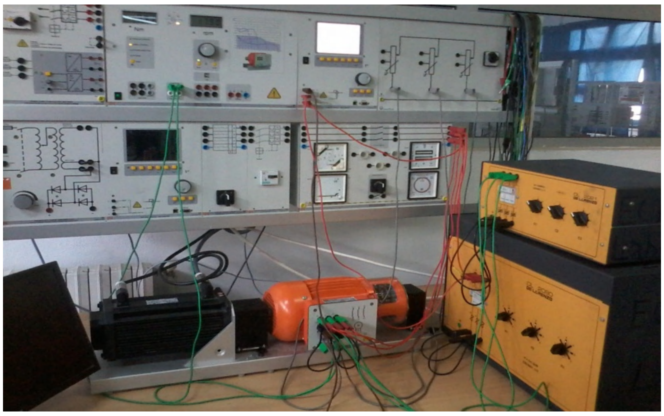

Fig.8. Experimental Bench

V. Conclusion

The main feature of the presented paper is the study of the operation, at constant frequency, of the wound rotor self excited induction generator. For various super-synchronous speeds, the frequency control is ensured by the addition of an external resistance to the rotor circuit. It is shown that, for a fixed capacity and constant frequency, the stator voltage is maintained constant, independent of speed and therefore remains sensitive only to the load impedance. Thus, the stator voltage drops when the load current increase despite the constancy of the frequency throughout the entire range of the speed.

The presented results have been compared by the corresponding experimental points. The close agreement between simulated and experimental points confirms the effectiveness of the presented method.

References

[1] Marc Bodson, *Fellow, IEEE*, and Oleh Kiselychnyk, "Analysis of Triggered Self-Excitation in Induction Generators and Experimental Validation", IEEE Trans. Energy Conversion, Vol. 27, No. 2, pp.238–249, June 2012.

[2] Kassa Idjdarene, Djamila Rekioua (ZIANI), Toufik Rekioua, and Abdelmounaim Tounzi, "Performance of an Isolated Induction Generator Under Unbalanced Loads", IEEE Trans. Energy Conversion, Vol. 25, No. 2, pp.303–311, June 2010.

[3] M. H. Haque, "A Novel Method of Evaluating Performance Characteristics of a Self-Excited Induction Generator, " IEEE Trans. Energy Conversion,Vol. 24, No. 2 ,pp.358–365, June 2009.

[4] K. Trinadha, and A. Kumar, "Performance of Wind Driven Induction Generator under Balanced/Unbalanced Load and Excitation," IEEE 2011.

[5] T. F. Chan, K. A. Nigim, L. L. Lai, "Voltage and Frequency Control of Self-Excited Slip-Ring Induction Generators, " *IEEE Trans. Energy* Conversion, vol. 19, pp.81–87, March. 2004.

[6] S. Singaravelu, S. Velusami, " Capacitive VAr requirements for wind driven self-excited induction generators," Energy Conversion and Management vol. 48 pp. 1367–1382, 2007.

[7] B. Singh, S. S. Murthy and S. Gupta, " STATCOM Based Voltage Regulator for Self Excited Induction Generator Feeding Non-Linear Loads," IEEE Trans. Ind. Electron., vol. 53, no. 5, pp. 1437–1452, October. 2006.

[8] L. Kalamen, P. Rafajdus, sekerák and V. Hrabovcová, " A Novel Method of Magnetizing Inductance Investigation of Self-Excited Induction Generators," IEEE transactions on magnetics, vol. 48 NO.4, pp. 1657–1660, 2007April 2012.

[9] D. Seyoum and C. Grantham, "Terminal voltage of a wind turbine driven isolated induction generator using stator oriented field control," IEEE Trans. Ind. App., pp. 846–852, 2003.

[10] Mateo Basic, Dinko Vukadinovic , " Vector control system of a self-excited induction generator including iron losses and magnetic saturation, " Control Engineering Practice 21 395–406, (2013).

[11] J. Breckling, Ghedamsi, K., & Aouzellag, D., " Improvement of the performances for wind energy conversions systems, " International Journal of Electrical Power & Energy Systems, 32, 936–945, (2010).

[12] M. Selmi, H. Rehaoulia, "A Simple Method for the Steady State Performances of Self-Excited Induction Generators, " ICEESA, 2013.

[13] Aissa Kheldoun ,Larbi Refoufi, Djalal Eddine Khodja, "Analysis of the self-excited induction generator steady state performance using a new efficient algorithm Electric Power Systems Research *86 61–67 (2012).*

[14] M. S. Miranda, R. O. Lyra and S. R. Silva, "An alternative isolated wind electric pumping system using induction machines", IEEE Trans. Energy Conversion, Vol. 14, No. 4, December 1999. pp. 1611-1616.

[15] E. G. Marra and J.A. Pomilio Grantham, "Self excited induction generator controlled by a VS-PWM bi-directional converter for rural applications," IEEE Trans. Ind. App., Vol. 1, 1998, pp. 116–122.